

# Active disturbance rejection control for looper tension of stainless steel strip processing line

**Dongyang Zhang, Qinghe Wu, Xiaolan Yao, Luliang Jiao**

*School of Automation, Beijing Institute of Technology, Beijing, 100081  
China (Tel: 182-1059-1943; e-mail: zhangdongyang2006@163.com,  
qinghew@bit.edu.cn, yaoxiaolan@bit.edu.cn, 747792472@qq.com)*

**Abstract:** In order to solve the tension disturbance problem of the strip processing line due to the motion of the looper carriage, the active disturbance rejection control (ADRC) strategy is presented. Meanwhile, the tension control of the looper is converted into the tension control of the wire rope between the winch and the looper carriage. A new tension measurement method is designed in order to obtain the tension and facilitate closed-loop tension control instead of a tension transducer. Considering the parameter uncertainty and the multi-disturbance of the stainless steel strip processing line, an ADRC controller is designed, and then the stability and parameter tuning procedure of ADRC are discussed. Finally, experiments are carried out based on the data from the processing line. Simulation results show the effectiveness of the proposed strategy.

**Keywords:** Looper, dynamics model, tension control, ADRC.

## 1. INTRODUCTION

Stainless steel strip processing line is a typical winding system. It usually includes the unwinder, the rewinder, the bridle, the looper, the processing segment, and the skin pass mill, etc. The main control objective of the stainless steel processing line is to keep the strip tension stable during the production process, especially in the processing segment. To maintain the logistics balance of rolling mill spans and the constant tension of the strip in the strip processing line, loopers are installed between rolling stands, and thus constitute an important element in the entire line (Seok, 1997). Motion of the looper carriage is facilitated by the change of strip velocity between the processing line and exit side of the looper. So the study of the dynamics and control strategy of the looper is a kind of important problem (Pagilla, 2001; Pagilla, 2003; Zhong, 2012) and is, therefore, the focus of this paper.

The study of the looper tension started only in recent years. A primary study on modelling and control of loopers was given in (Pagilla, 2001); an average dynamic model was developed and used for control design. Then various advanced control strategies were proposed and applied to solve this problem, such as Lyapunov's second method (Pagilla, 2003), sliding-model control (Zhong, 2012), decentralized robust decoupling control (Yang, 2015), and differential geometry control (Noh, 2011). A discrete-time fuzzy state feedback control was proposed for looper tension control in (Chen, 2012). These methods enriched the theory research of the looper tension control. However those methods are complicated based on the accurate system models or the information of disturbance, so that they are difficult to implement in the engineering. In the actual engineering, PI

control (Magura, 2016; Yang, 2017; Gan, 2017; Yin, 2018; Mao, 2018) and the open-loop control are generally adopted. In (Yang, 2017), it set up a tensiometer to measure the strip tension, however, it increased the cost. In (Yin, 2018), it improved the process, while it also increased the cost. Furthermore, PI controller cannot meet all requirements of the control objects and specifications. Without a feed-back in the open-loop control, it will produce a wobble to the tension inevitably (Wang, 2004). Therefore, to further improve the quality and efficiency in industry, researchers and engineers try to explore better methods for the tension control.

The emergence of active disturbance rejection control (ADRC) brings a new way to solve the looper tension control problem (Huang, 2012). ADRC can actively estimate and reject disturbances of both internal and external disturbances, which is independent of models and more suitable for the nonlinear system theoretically. And ADRC has been applied to many systems (Liu, 2011; Pedro, 2013; Sira-Ramirez, 2014; Jiang, 2015; Li, 2015; Guo, 2016; Zhou, 2017). (Zhou et al., 2007) has applied ADRC to the tension control of loopers firstly. Then (Zhang et al., 2014) applied ADRC to the winding system. Based on that, considering characteristics of the looper, this paper translates the tension control of the looper into the wire rope tension between the winch and the looper carriage in modelling the tension dynamic model of the looper. Then a new tension measurement method and an ADRC controller are designed. In order to validate the effectiveness of the proposed strategy, results of the tension measurement module is compared with the actual tension value, and results of the ADRC controller is compared with the PI controller and the open-loop control.

In this paper, the main contribution of this study is given by:

- 1) Convert the looper tension control into the tension control of the wire rope between the winch and the looper carriage first time, so that it simplified the control model greatly;
- 2) Replace the tension transducer with a new linear tension measuring method, in order to decrease the cost and the complexity of structure;
- 3) Design an ADRC controller to control the looper tension and adopt the actual industrial data to do experiments. So it can reflect the value of the proposed approach in industrial field.

The reminder of this paper is organized as follows. Section 2 analyses the structure of the looper and builds its dynamics model. Section 3 designs a new tension measurement method. An ADRC controller is designed to control the tension, and then the stability and parameter tuning of ADRC are discussed in section 4. Simulation experiments are discussed in section 5. Section 6 gives concluding remarks.

## 2. TENSION DYNAMIC MODEL

### 2.1 Analysis of looper structure

The looper mainly consists of upstream rollers, downstream rollers, a looper carriage, and the driven device. The number of rollers in a looper is determined by the quantity of strip steel to be stored and the length or height of the looper. The driven device consists of the wire rope and a winch which

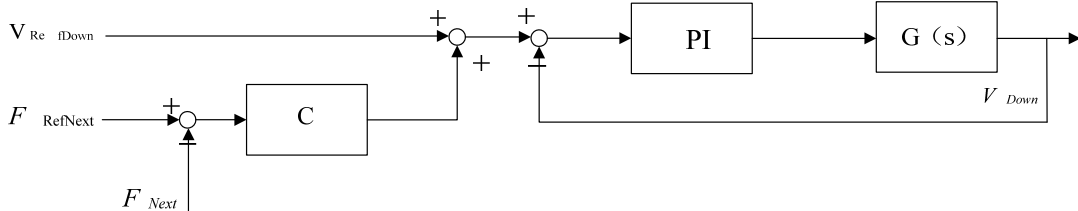


Fig. 2. Sketch of downstream driven roller.

The winch control adopts the open-loop control in industry, that is, the winch pulls the carriage with a constant force. Due to the friction between the carriage and the ground or bearings, the direction of the friction will change with the reversing motion of the carriage. When the speed of the looper carriage is positive, the force equation is given by:

$$nF_{Looper} + f = 2F_{Rope} \quad (1)$$

When the speed of the looper carriage is negative, the force equation is given by:

$$nF_{Looper} - f = 2F_{Rope} \quad (2)$$

where,  $F_{Looper}$  is the tension of the looper,  $f$  is the friction of the looper carriage, and  $n$  is the layer number of the strip.

Notice that  $F_{Rope}$  is constant, so  $F_{Looper}$  will increase with the reversing motion of the looper carriage. Thus, the motion of the looper carriage will lead a large disturbance to the tension control.

provides power for the operation of loopers. A simplified schematic of a looper is shown in Fig.1.

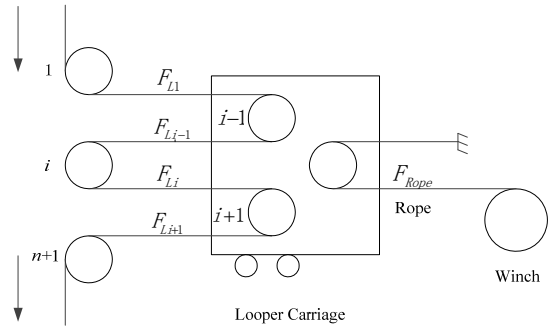


Fig. 1. Sketch of a looper.

In Fig. 1,  $F_{Li}$  is the strip tension of the  $i^{th}$  layer;  $F_{Rope}$  is the wire rope tension. Generally, the speed of upstream driven rollers is the reference of the entire looper section; the speed of downstream driven rollers needs to be corrected in real time according to the tension error between the reference of the current span and the actual tension of the next adjacent span, as shown in Fig. 2. In Fig. 2,  $v_{Re\_fDown}$  is the reference velocity of downstream driven rollers,  $v_{Down}$  is the actual velocity of downstream driven rollers,  $F_{Re\_fNext}$  is the reference tension of the next span,  $F_{Next}$  is the actual value of the next adjacent tension span.

### 2.2 Looper tension dynamic model

According to (Pagilla, 2001), the average tension of the looper is given by:

$$F_{Looper} = \frac{1}{n} \sum_{i=1}^n F_i \quad (3)$$

when the looper carriage speed is constant, if the friction is ignored, the relationship between the average tension of the strip in looper and the wire rope tension is given by:

$$F_{Looper} = \frac{2}{n} F_{Rope} \quad (4)$$

Because of the constant quantitative relationship between the rope tension and the looper average tension, the looper tension control is converted into the rope tension control between the winch and looper carriage. According to the theory in (Pagilla, 2001), we seem the system of the winch, wire rope and carriage as a span on the processing line. In Fig. 1, the connection part of the rope and carriage is equivalent to a movable pulley, and the sliding friction force

is ignored. The relationship between the speed of the winch and looper carriage is given by

$$\frac{1}{2} v_w = v_c \quad (5)$$

where,  $v_w$  and  $v_c$  are the velocity of the winch and the looper carriage, respectively. That is the carriage and the winch are equivalent to the  $j^{th}$  roller and the  $(j+1)^{th}$  roller, respectively. The wire rope is fixed at one end and the winch has just one end, that is,  $\omega_{j-1} = 0$ ,  $F_{j+1} = 0$ . Then the wire rope tension dynamics and the speed dynamics of the winch are given by:

$$\frac{dF_{Rope}}{dt} = \frac{E_0 A}{L_{Rope}(t)} (v_w + d \frac{dv_w}{dt}) - \frac{F_{Rope}(t)}{L_{Rope}(t)} v_w \quad (6)$$

$$J \frac{dv_w}{dt} = RT_q - R^2 F_{Rope}(t) \quad (7)$$

where,  $E_0$ --modulus of elasticity of the wire rope;

$A$ --area of cross-section of the wire rope;

$L_{Rope}(t)$ --length of the wire rope(a variable);

$R$ --radius of the winch;

$v_w$ --speed of the winch ( $= \omega_w R$ );

$J$ --moment of inertia of the winch;

$v_c$ --speed of the looper carriage;

$d$ --damping coefficient;

$T_q$ --torque of the output motor;

Notice that (6) does not meet the superposition principle, and there is a highly coupling between the rope dynamics (6) and

speed dynamic (7), which shows the tension dynamics is sensitive to speed variations.

### 3. TENSION MEASUREMENT

To obtain the real-time tension, it usually installs a tension transducer in industry. But it will increase the hardware cost and system complexity. So in this paper we proposed a new method to measure the actual tension.

The tension measurement for the winch system has been studied by many researchers, such as the frequency-based tension measuring method (Song, 2000) and the nonlinear tension measuring method (Lynch, 2004), etc. Based on that, in this section, a linear tension measuring method is designed according to the model of the tension dynamics, which structure is simple and easy to implement. Section 5 will do some simulations to test its accuracy.

Because  $L_{Rope}(t)$  is time-varying with the movement of the looper carriage, the analytic equation of the rope tension cannot be conducted according to the rope dynamics (6). While according to (7), it can be rewritten as:

$$F_{Rope} = -\frac{J}{R^2} \dot{v}_w + \frac{1}{R} T_q \quad (8)$$

that is the tension measuring method.

### 4. ADRC DESIGN

#### 4.1 Design process of ADRC controller

The speed dynamics (7) has a good linearity, and practices in industry show that PI control has met requirements of rapidity and accuracy, so the speed loop applies PI control. And the tension is controlled via ADRC. So the control of the rope tension and winch speed forms a cascade control, as shown in Fig. 3.

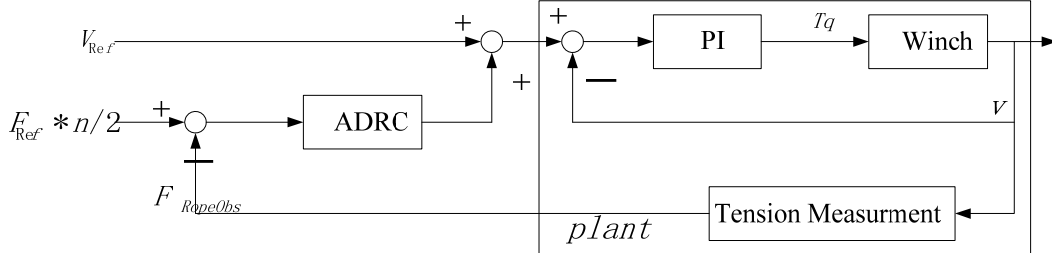


Fig. 3. Sketch of the carriage control.

In Fig. 3,  $F_{Ref}$  is the reference value of the looper tension;  $F_{Ref} * n/2$  is the corresponding reference value of the rope;  $v_{Ref}$  is the speed reference value. If  $v_{RefUp}$  is the reference value of upstream driven rollers and  $v_{RefDown}$  is the reference value of downstream driven rollers;  $n$  is the layer number of the strip;  $v_{Ref}$  is given by:

$$v_{Ref} = \frac{v_{RefDown} - v_{RefUp}}{n/2} \quad (9)$$

In (6) and (7), the length of the rope is time variables, and the first-order ADRC cannot make the system stable tested by actual industrial sites. So this paper adopts the two-order ADRC.

In order to facilitate the design of the ADRC, we do derivation to the (6) and (7) (Note that, for simplicity,  $F_R = F_{Rope}$ ,  $L_R = L_{Rope}$ ),

$$\ddot{F}_R = \frac{E_0 A L_R (\dot{v}_w + d \ddot{v}_w)}{L_R^2} - \frac{E_0 A (v_w + d \dot{v}_w) \dot{L}_R}{L_R^2} - \frac{(\dot{F}_R v_w + F_R \dot{v}_w) L_R - F_R v_w \dot{L}_R}{L_R^2} \quad (10)$$

$$\ddot{v}_w = -R^2 \dot{F}_R / J \quad (11)$$

Then substitute (7) and (11) to (10)

$$\begin{aligned} \ddot{F}_R &= \frac{E_0 A}{L_R J} (RT_q - R^2 F_R) - \frac{E_0 A d R^2}{L_R J} \dot{F}_R - \frac{E_0 A \dot{L}_R}{L_R^2} v_w \\ &\quad - \frac{E_0 A d \dot{L}_R}{L_R^2 J} (RT_q - R^2 F_R) - \frac{v_w}{L_R} \dot{F}_R \\ &\quad - \frac{F_R v_w}{L_R J} (RT_q - R^2 F_R) + \frac{F_R v_w}{L_R^2} \dot{L}_R \end{aligned} \quad (12)$$

According to Fig.3, it can be obtained that the tension and the speed compose a cascade system. So let the speed  $v_w$  as the control volume,  $u = v_w$ . In order to facilitate the design of the controller, the (12) is linearized at the working point  $(\bar{F}_R, \bar{v}_w)$ , and described in the following form

$$\ddot{F}_R = P(t) + bu \quad (13)$$

Where  $b = -\frac{E_0 A \dot{L}_R}{L_R^2} - \frac{\bar{F}_R}{L_R} + \frac{\bar{F}_R}{L_R^2} \dot{L}_R$ ,  $P(t) = d + \hat{f}(t)$  denotes the total disturbance ( $d$  is the external disturbance and  $\hat{f}(t)$  is the internal unknown disturbance.):

$$d = \frac{E_0 A R T_q}{L_R J} - \frac{E_0 A d \dot{L}_R R T_q}{L_R^2 J} \quad (14)$$

$$\begin{aligned} \hat{f}(t) &= -\frac{E_0 A R^2}{L_R J} F_R - \frac{E_0 A d R^2}{L_R J} \dot{F}_R + \\ &\quad \frac{E_0 A d \dot{L}_R R^2}{L_R^2 J} F_R - \frac{\bar{v}_w}{L_R} \dot{F}_R + \\ &\quad \frac{\bar{v}_w \dot{L}_R}{L_R^2} F_R - \frac{R T_q}{L_R J} F_R + \frac{R^2}{L_R J} F_R^2 \end{aligned} \quad (15)$$

The value of  $b$  cannot be determined, so this paper introduces the adjustable parameter  $b_0$  that is the estimated value of  $b$ . Taking  $f(t) = P(t) + (b - b_0)u$  as the total disturbance which is a bounded value, and the Eq.(13) can be rewritten as:

$$\ddot{F}_{\text{rope}} = P(t) + bu = f(t) + b_0 u \quad (16)$$

This is the controlled object which is approximated to a two-order model. Then let  $x_1 = F_R$ ,  $x_2 = \dot{F}_R$ ,  $x_3 = f$ ,  $h = \dot{f}$ ,  $y = F_R$ , we can obtain the extended state space equation, that is given by

$$\begin{aligned} \dot{x} &= Ax + Bu + Eh \\ y &= Cx \end{aligned} \quad (17)$$

$$\text{Where } A = \begin{bmatrix} 0 & 1 & 0 \\ 0 & 0 & 1 \\ 0 & 0 & 0 \end{bmatrix}, B = \begin{bmatrix} 0 \\ b_0 \\ 0 \end{bmatrix}, E = \begin{bmatrix} 0 \\ 0 \\ 1 \end{bmatrix}, C = [1 \ 0 \ 0].$$

In order to reduce controller parameters, linear ADRC is designed. That is, the linear state error feedback (LSEF) and the linear extended state observer (LESO) are applied (Huang, 2012), as shown in Fig. 4.

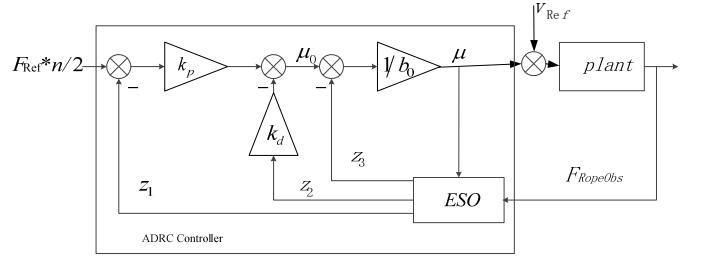


Fig. 4. Sketch of ADRC.

ESO is used to estimate states and total disturbances; the controlled input  $u$  and the output of the tension measurement module  $F_{\text{RopeObs}}$  are inputs of ESO. Let  $y = F_{\text{RopeObs}}$ , then ESO is given by:

$$\begin{cases} \dot{z}_1 = z_2 + \beta_1(y - z_1) \\ \dot{z}_2 = z_3 + \beta_2(y - z_1) + b_0 u \\ \dot{z}_3 = \beta_3(y - z_1) \end{cases} \quad (18)$$

where,  $z_1$ ,  $z_2$ ,  $z_3$  are estimate values of system states and the total disturbance,  $y$ ,  $\dot{y}$  and  $f$ , respectively; and  $\beta_1, \beta_2, \beta_3$  are parameters of ESO.

The LSEF adopts the PD control, because the total disturbance is compensated timely by the variable  $z_3 / b_0$ , which can eliminate the static error and avoid the negative effect of the integral negative feedback. The state error feedback law and the disturbance compensation is given by:

$$\begin{aligned} u_0 &= k_p(F_{\text{Ref}} * n/2 - z_1) - k_d z_2 \\ u &= \frac{u_0 - z_3}{b_0} \end{aligned} \quad (19)$$

where,  $k_p, k_d, b_0$  are parameters of the controller.

#### 4.2 Stability analysis of ADRC

The stability is the precondition of analyzing and designing a normally working system, and it can guide the parameter setting. The stability of LADRC has been studying in recent years (Chen, 2013; Gao, 2003). Then we will prove the stability of ADRC applied in this paper.

The system has been approximated to a second-order model and transformed into the extended state space equation, as shown in (16) and (17). Then combine it with (18), the error equation is

$$\dot{e} = A_e e + Eh \quad (20)$$

where,  $e$  is the estimate error of ESO,  $e_i = z_i - x_i$ , and  $A_e = \begin{bmatrix} -\beta_1 & 1 & 0 \\ -\beta_2 & 0 & 1 \\ -\beta_3 & 0 & 0 \end{bmatrix}$ . Obviously, LESO is bounded-input

bounded-output (BIBO) stable if roots of the characteristic polynomial of  $A_e$ ,  $\lambda(s) = s^3 + \beta_1 s^2 + \beta_2 s + \beta_3$ , are all on the left half plan and  $h$  is bounded.

According to (19), the state feedback is given by

$$u = (1/b_0) [(-k_p z_1 - k_d z_2 - z_3) + k_p r] \quad (21)$$

where,  $r$  is the reference input  $F_{ref} * n/2$ . Then the closed-loop system is represented by

$$\begin{bmatrix} \dot{x} \\ \dot{z} \end{bmatrix} = \begin{bmatrix} A & \bar{B}F \\ LC & A - LC + \bar{B}F \end{bmatrix} \begin{bmatrix} x \\ z \end{bmatrix} + \begin{bmatrix} [\bar{B} & E] \\ [\bar{B} & 0] \end{bmatrix} \begin{bmatrix} r \\ h \end{bmatrix} \quad (22)$$

where,  $\bar{B} = B/b_0$ ,  $L = [\beta_1 \ \beta_2 \ \beta_3]$ ,

$$F = (1/b_0) [-k_p \ -k_d \ -1]$$

Obviously, the closed-loop system is bounded-input bounded-output (BIBO) stable if its eigenvalues are in the left half plan. The closed-loop eigenvalues satisfy

$$\begin{aligned} & \text{eig} \left( \begin{bmatrix} A & \bar{B}F \\ LC & A - LC + \bar{B}F \end{bmatrix} \right) \\ &= \text{eig} \left( \begin{bmatrix} A + \bar{B}F & \bar{B}F \\ 0 & A - LC \end{bmatrix} \right) \\ &= \text{eig}(A + \bar{B}F) \cup \text{eig}(A - LC) \end{aligned} \quad (23)$$

that is, the stability of the closed-loop system is determined by two characteristic polynomials

$$\begin{aligned} \lambda_1(s) &= s^3 + \beta_1 s^2 + \beta_2 s + \beta_3 \\ \lambda_2(s) &= s^2 + k_d s + k_p \end{aligned} \quad (24)$$

For simplicity, we make that

$$\begin{aligned} s^3 + \beta_1 s^2 + \beta_2 s + \beta_3 &= (s + \omega_o)^3 \\ s^2 + k_d s + k_p &= (s + \omega_c)^2 \end{aligned} \quad (25)$$

So the convergence of LESO and ADRC is determined by  $\omega_o$  and  $\omega_c$ .

#### 4.3 Parameters regulation of ADRC

Firstly, according to (25),  $k_p$ ,  $k_d$  are given by:

$$k_p = \omega_c^2, \ k_d = 2\omega_c \quad (26)$$

When ESO works well,  $z_1 \approx y$ ,  $z_2 \approx \dot{y}$ ,  $z_3 \approx f$ , substituting (19) to (16), yields  $\ddot{y} \approx u_0$ , that is the control system is converted into a cascaded integral form.

Substituting (19) to  $\ddot{y} \approx u_0$ , the expected closed-loop system is

$$\ddot{y} + k_d \dot{y} + k_p y = k_p r \quad (27)$$

then the transfer function is

$$\begin{aligned} G_c(s) &= \frac{Y(s)}{r(s)} = \frac{k_p}{s^2 + k_d s + k_p} \\ &= \frac{\omega_c^2}{(s + \omega_c)^2} \end{aligned} \quad (28)$$

The overshoot is zero according to (28). So the main purpose is to choose the appropriate control bandwidth to obtain the satisfying setting time (The conclusion can be seen in (Chen, 2013)). According to the definition of the setting time (Gao, 2003),  $t_s \approx 5.85/\omega_c$ ,  $k_p$ ,  $k_d$  can be adjusted according to (26).

Although a large number of simulation experiments show the stability region will increase with the increasing of  $b_0$  (Chen, 2008), it cannot be too large, or it will make the control signal too small to lead to respond slowly. So the tuning of  $b_0$  is a weighting process of the stability (robustness) and response speed.

Secondly, according to [17],  $\beta_1, \beta_2, \beta_3$  are given by:

$$\beta_1 = 3\omega_o, \ \beta_2 = 3\omega_o^2, \ \beta_3 = k\beta_2 \quad (29)$$

Generally, when  $t_s > 1s$ ,  $k = 4$ ,  $\omega_o$  has a minimal effect to the observed speed of ESO. So  $\omega_o$  can be given by  $\omega_o = 4\omega_c$ .  $\beta_1, \beta_2, \beta_3$  are obtained according to (29).

In conclusion, the parameter tuning procedure of the second-order ADRC is followed as:

- 1)  $k_p$ ,  $k_d$  are calculated by (26) based on  $t_s$ ;
- 2)  $\beta_1, \beta_2, \beta_3$  are calculate by (29) based on  $\omega_o$ ;
- 3)  $b_0$  is tuned recurrently base on the actual process until meeting system requirements.

## 5. EXPERIMENTAL RESULTS

The entry looper of the cold-rolled annealing and pickling line of stainless steel strip processing line of some company is taken as an example. All driven rolls have been done friction loss test, which is the basis of the friction load compensation during the control process. And all mechanical and electrical parameters of the simulation example completely come from the processing line and have been validated in processing line and simulation of step response. And the data for disturbance test are collected from the worksite. Fig.5 shows a schematic of the bridle unit of the entry looper.

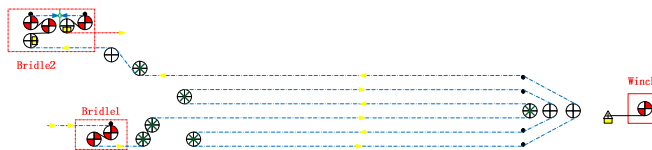


Fig. 5. Structure of entry looper bridle unit.

The looper is located between the 1st bridle and 2nd bridle, containing six layers strip steel. The 1st bridle, which contains two driven rollers and connects the unwinder with the looper, locates at the entrance of the entry looper, and its velocity is the reference value in the entire processing line.

The 2nd bridle, which contains two driven rollers and two idle rollers and connects the continuous annealing section with the looper, locates at the export of the entry looper and transports strip to the annealing furnace in a constant velocity. Parameters of the stainless steel strip are shown in table 1, and the main mechanical and electrical parameters of the driven rolls are shown in table 2.

**Table 1. Parameters of stainless steel strip.**

	cross-section area	elastic modulus	density
Value	1.81E-03 $m^2$	2.06E+11 Pa	8710 Kg / m <sup>3</sup>

**Table 2. Mechanical and electrical parameters.**

	rotary inertia/kgm <sup>2</sup>	roll diameter/m	gear ratio -	wrap angle dgree	nominal torque Nm	rated power/kw	nominal speed/rpm
Roll 1.1	5	1	19.4000	10	722.755	75	991
Roll 1.2	6	1	19.9079	11	962.702	100	992
Roll 2.1	1.94	1	32.5275	10	359.461	37	983
Roll 2.2	1.65	1	31.5986	11	213.516	22	984
Roll 2.3	1.75	1	32.5986	12	179.365	18.5	985
Winch Roll	11.25	1.45	101.26	11	1540.323	160	992

### 5.1 Simulation results of tension measurement

Under the open-loop control, this section tests the effect of the tension measurement method from two aspects.

#### (1) Speed disturbance

The reference tension of the looper is 33626N. That is the reference tension of the rope is 100878N. The reference speed of the 1st bridle decreases from 327.274rpm to 62rpm in Fig. 6(a); the speed of the 2nd bridle keeps constant. So the looper begins to unwind at this time. According to (9), the speed of the winch is shown in Fig. 6(b), which decreases from 288.96rpm to 0 and increase to 28.245rpm reversely. Fig. 7 shows the comparison between the observed value and the actual tension under open-loop control.

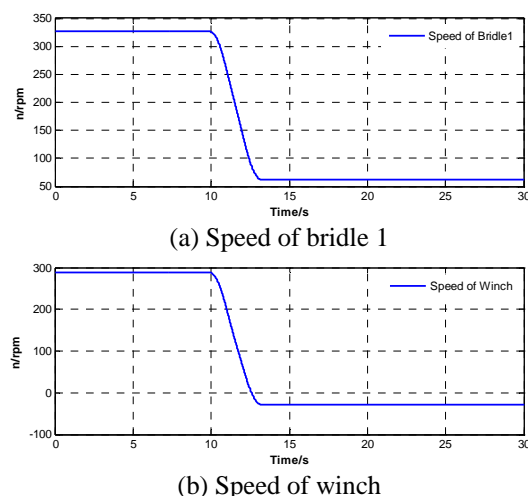


Fig. 6. Speed of upstream rollers and winch.

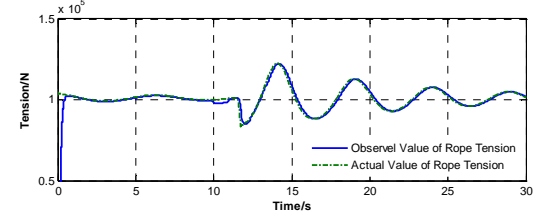


Fig. 7. Results of tension measurement module.

According to Fig. 7, it turned out that the tension measurement method can track the actual tension well. The results also shows that the tension has about 21.4% overshoot when the winch speed crosses zero and it needs about 17.5s to adjust. So we can conclude that the anti-interference ability of the open-loop control is poor.

#### (2) Tension disturbance

Keeping the 1st bridle reference speed at 327.274rpm, the looper tension reference value is shown in Fig.8, jumping from 33626N to 35626N. Fig. 9 shows the results of the comparison between the observed value and the actual tension under open-loop control.

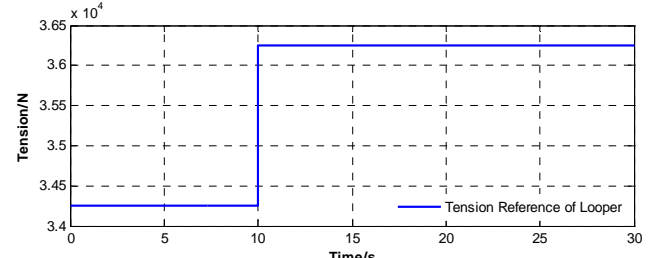


Fig. 8. Looper tension reference value.

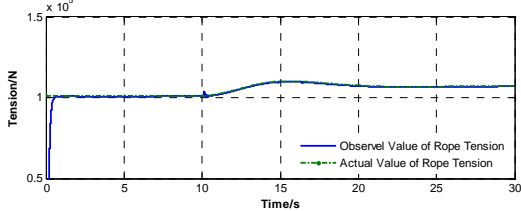


Fig. 9. Results of tension measurement module.

According to Fig.9, it turned out that the tension measurement method can track the actual tension well. And at the instant of tension changing suddenly, the setting time is about 5s. So we also can conclude that the response speed of the open-loop control is slower.

Base on the above results, the tension measurement method is effective and accurate.

### 5.2 Simulation results of tension control

The reference tension of looper is 33626N. Following the parameter regulating procedure described in section 4.3, parameters of the design are shown in table 3.

**Table 2. Parameters of ADRC and PI controller.**

Values of the gains used in the simulation	
PI	$k_p = 1.0 \times 10^{-4}$ $k_i = 0.033$
ADRC	$\omega_0 = 90$ $\omega_c = 50$ $b_0 = 1.0 \times 10^8$

Then the expected transfer functions of LESO and the closed-loop system are given respectively by

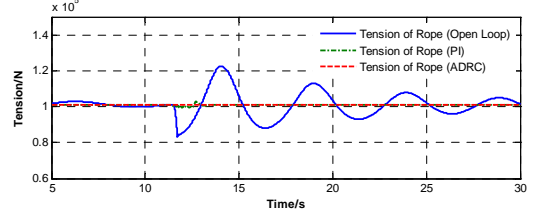
$$G_c(s) = \frac{2500}{s^2 + 100s + 2500} \quad (30)$$

$$G_o(s) = \frac{97200}{s^3 + 270s^2 + 24300s + 97200} \quad (31)$$

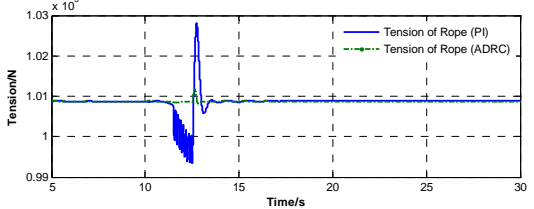
The cutoff frequency of LESO and the closed-loop system are 46.37 rad/s (7.38Hz) and 32.19 rad/s (5.12Hz), respectively. So we can conclude that there is no problem about sampling frequency on the implementation of ADRC controller.

Then this part will analyze the tension controlled via the proposed method. Due to the page limit, this part just selects the speed in Fig. 6 as the tension disturbance. The friction of the carriage brought by the inverse of winch speed leads a large disturbance to the rope tension.

Fig. 10 shows results of rope tension control. The result demonstrates that the open-loop control has a bad anti-disturbance ability. When giving a disturbance, it has a large overshoot and a long time to adjust. PI control and ADRC have a better anti-disturbance ability. Fig. 10(b) shows that ADRC can restrain the disturbance peak at 0.29% of the reference tension, and it just need 0.3s to adjust. While PI control restrain the disturbance peak at 1.9% of the reference tension, and it need about 2.5s to adjust. So we can conclude that ADRC has a stronger anti-disturbance ability than PI control and the open-loop control.



(a) Rope Tension Control by Open-loop, PI and ADRC



(b) Amplifying Rope Tension Control by PI and ADRC

Fig. 10. Rope tension control curve.

Fig. 11 shows the looper tension control. They are almost entirely coincidence with the Fig. 10(a). So a detailed analysis is omitted. ADRC has the smallest overshoot and settling time when giving a disturbance.

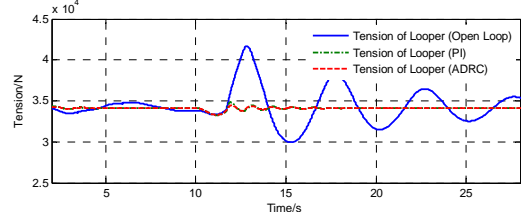
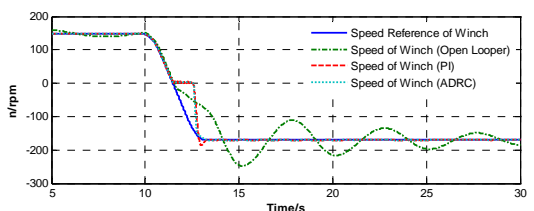
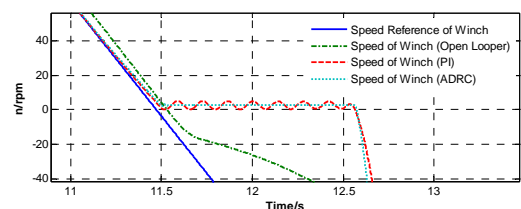


Fig. 11. Looper tension control of the open-loop, PI and ADRC.

The winch speed is shown in Fig. 12. When the reference speed of winch cross zero, the speed of the open-loop control has a great fluctuation and it need about 17.5s to adjust. While the settling time of PI and ADRC are about 2s and 1.5s, respectively; and PI control has a 16.7% overshoot. Furthermore, from Fig. 12(b), after adding the disturbance, PI control has a fluctuation. Thus, the control effect of ADRC is better than PI control obviously.



(a) Winch Speed by Open-loop, PI and ADRC



(b) Amplifying Winch Speed

Fig. 12. Winch speed.

The speed curves of looper carriage are shown in Fig.13. The control effect is similar with the winch speed. So a detailed analysis is omitted. Obviously, ADRC is the best control method.

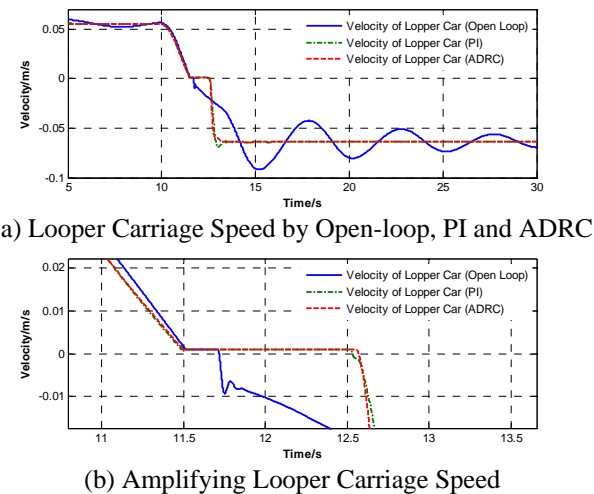


Fig. 13. Looper carriage speed.

Furthermore, from Fig.12, the initial value of  $\omega_w$  is about 158 n/rpm. Then according to (5), the line speed of the carriage is 0.0573 m/s. From Fig.13, the initial value of  $v_c$  is 0.0580 m/s. The tolerance between the actual speed and the calculated speed is 0.0007 m/s.

In sum, the proposed modelling strategy is effective and accurate according to results of Fig. 10, Fig. 11, Fig. 12 and Fig. 13. The ADRC controller is better than the open-loop control and PI control, and ADRC controller has a strong anti-disturbance ability.

**Remark1:** Compared with (Zhou, 2007), this paper has two advantages:

### 1) In modelling

In this paper we converted the looper tension control into the control of the wire rope tension between the winch and the looper carriage, and then replace the tension meter by a new tension measurement method. During modelling, it avoided to consider the elasticity and uniformity of the strip and the dynamics of the tension meter and idle rollers (Zhou, 2007). So this method is simple for modelling and easy to analyse the characteristics of the system and design a controller.

### 2) Simulation results

In (Zhou, 2007), the velocity loop and the tension loop both applied the ADRC, while in this paper the velocity loop and the tension loop applied the PI control and the ADRC, respectively. The PI control is easy to design and tune parameters. And we apply the field data to simulate in order to be more accurate and satisfy the actual application than (Zhou, 2007). Furthermore, as to the velocity loop, according to simulation results, the control effect of PI control is better than the ADRC under the open-loop condition. Under the closed-loop condition, the winch and the looper velocity controlled by ADRC in this paper only have a small

fluctuation when the velocity crosses zero; in (Zhou, 2007), it has a tracking error when the desired velocity changes.

Overall, we can conclude that the proposed method in this paper is effective and valuable for future study about the looper control.

## 6. CONCLUSIONS

This paper presents an application study of ADRC in solving the looper tension control problem of the stainless steel strip processing line. In order to simplify the control design, the looper tension control is converted into the tension control of the wire rope between the winch and the looper carriage. Then a new tension measurement method and a second-order ADRC for the tension loop are designed. Meanwhile, the stability conditions and parameter tuning procedure are discussed. Finally, it takes the looper of the pickling section of the stainless steel strip processing line as an example. Results of the measured tension show that the tension measurement method can track the actual tension well and completely replace the tension meter theoretically; results of tension control experiments show that the proposed design is effective, and ADRC does a much better job at rejecting the disturbances than the open-loop control and PI control.

## REFERENCES

- Chen J X, Zhang Y G, Yu L Y. (2012). Discrete-time fuzzy state feedback control for looper and tension control systems, *Proceeding of International Conference on mechatronics and Automation, IEEE, Chengdu, China, 5-8 August, 2012* (pp.2590-2594).
- Chen X. (2008). Active Disturbance Rejection Control Tuning and Its Application to Thermal Processes. *Beijing: Tsinghua University*.
- Chen Z.Q, Sun M.W, Yang R. (2013). On the Stability of Linear Active Disturbance Rejection Control. *Acta Automatica Sinica*, 39(5), 574--580.
- Gan S Q, Huang S, Xue Y Z, Zhang H. (2017). Looper control of cold rolling continuous annealing production line, *Metallurgical Automation*, (S1), 173-176.
- Gao Z.Q. (2003). Scaling and bandwidth-parameterization based controller tuning. *American Control Conference, Denver, Colorado , 4--6 June 2003* (pp.4989--4996).
- Guo B.Z, Wu Z.H, Zhou H.C. (2016). Application of Linear Active Disturbance Rejection Controller for Sensorless Control of Internal Permanent-Magnet Synchronous Motor. *IEEE Trans. on Automatica Control*, 61(6), 1613-1618.
- Huang Y, Xue W.C. (2012). Active disturbance rejection control: thought, application and theoretical analysis, *System Science & Math Science*, 32(10), 1287--1307.
- Jiang T.T, Huang C.D, Guo L. (2015). Control of uncertain nonlinear systems based on observers and estimators. *Automatica*, 59, 35--47.
- Li H., Liu X.Q., Li J. (2015). The research of Fuzzy Immune Linear Active Disturbance Rejection Control Strategy for three-motor synchronous system, *Journal of Control Engineering and Applied Informatics*, 17(4) , 50-58.
- Liu X.Q., Tang L., Zhou L. (2011). Fuzzy Active Disturbance Rejection Control of Three-Motor

- Synchronous system. *Journal of Control Engineering and Applied Informatics*, 13 (4), 51-57.
- Lynch A.F, Bortoff S.A, Röbenack K.R. (2004). Nonlinear tension observers for web machines. *Automatica*, 40(9), 1517--1524.
- Magura D, Fedák V, Kyslan K, et al. (2016). Practical experience with control of drives of an accumulator in a web processing continuous line, *International Conference on Mechatronics - Mechatronika. IEEE, Prague, Czech Republic, 7-9 Dec, 2016*.
- Mao X, Zhi S Q. (2018). Decoupling control strategy for multi-tower vertical looper, *Metallurgical Industry Automation*, 42(3), 37-41.
- Noh I, Won S, Jang Y.J. (2011). Non-interactive Compensation in Entire State Domain for Looper Tention Control System. *11th Int. Conf. on Control, Automation & Systems, Gyeonggi-do, Korea, 26--29 Oct. 2011* (pp.1269--1273).
- Pagilla P.R, Garimella S.S, Dreinhoefer L.H, et al. (2001). Dynamics and control of accumulators in continuous strip processing lines. *IEEE Trans. on Industry Applications*, 37(3), 934--940.
- Pagilla P.R, Singh I, Dwivedula R.V. (2003). A study on control of accumulators in web processing lines. *in Proc. of American Control Conference, Oenver, Colorado, 4--6 June 2003* (pp.3684--3689).
- Pedro T G, Germain G. (2013). Optimal Tuning of PI/PID/PID(n-1) Controllers in Active Disturbance Rejection Control, *Journal of Control Engineering and Applied Information*, 15(4), 26-36.
- Seok, J.K, Chung D.W, Song S.H, et al. (1997). A new approach to advanced cold mill drive systems. *in IEEE Industry Application Conference, New Orleans, USA, 5--9 Oct. 1997* (pp.2125--2130).
- Sira-Ramirez H, Castro-Linares R, Puriel-Gil G. (2014). An Active Disturbance Rejection Approach to Leader-Follower Controlled Formation. *Asian Journal of Control*, 16(2), 382--395.
- Song S.H, Sul S.K. (2000). A new tension controller for continuous strip processing line. *IEEE Trans. On Industry Applications*, 36(2), 633--639.
- Wang C.X, Wang Y.Z, Yang R.Q, et al. (2004). Research on precision tension control system based on neural network. *IEEE Trans. on Industrial Electronics*, 51(2), 381--386.
- Yang X D, Fu Z Z. (2017). Study on Dynamic Compensation of Vertical Looper in Cold Rolling & Galvanizing Mill, *ANGANG TECHNOLOGY*, (5), 35-39.
- Yang Z, Liu D, Chao X.L, Wang R, Qian F.C, Zheng G. (2015). Decentralized robust decoupling control for looper tension and height system. *Proceedings of the 34th Chinese Control Conference, Hangzhou, China, 28-30 July 2015* (pp.326--331).
- Yin N. (2018) Study and improvement on looper tension control of hot-dip galvanizing unit, *Science and Technology &Innovation*, (4), 123-124.
- Zhang W, Cai Y, Deng B, et al. (2014). *Active Disturbance Rejection Control for Tension Regulation of Stainless Steel Strip Processing Line[J]. In: Wen Z, Li T. (eds) Practical Applications of Intelligent Systems. Advances in Intelligent Systems and Computing*, 279, 47-57.
- Zhong Z.Z, Wang J.C, Zhang J.M, et al. (2012). Looper-Tenstion Sliding Mode Control for Hot Strip Finishing Mills. *Journal of Iron and Steel Research (Intrenational)*, 19(1), 23--30.
- Zhou W.K, Gao Z.Q. (2007). An active disturbance rejection approach to tension and velocity regulations in web processing lines. *IEEE Int. Conf. on Control Applications, Singapore, 1-3 Oct. 2007* (pp.842--848).
- Zhou Y L, Wang D, Qi T Y. (2017). Modelling, Validation and Control of Steam Turbine Bypass System of Thermal Power Plant, *Journal of Control Engineering and Applied Informatics*, 19(3), 41-48.